











RESEARCH ARTICLE

Digital diaphanoscopy of maxillary sinus pathologies supported by machine learning

Ekaterina O. Bryanskaya¹  | Viktor V. Dremin¹  | Valery V. Shupletsov¹  |
Alexey V. KornaeV²  | Mikhail Yu. Kirillin^{3,4}  | Anna V. Bakotina⁵  |
Dmitry N. Panchenkov⁵  | Konstantin V. Podmasteryev¹  |
Viacheslav G. Artyushenko⁶  | Andrey V. Dunaev¹ 

¹Research and Development Center of Biomedical Photonics, Orel State University, Orel, Russia

²Research Center for Artificial Intelligence, Innopolis University, Innopolis, Russia

³Institute of Applied Physics RAS, Nizhny Novgorod, Russia

⁴N.I. Lobachevsky State University of Nizhny Novgorod, Nizhny Novgorod, Russia

⁵Yevdokimov A.I. Moscow State University of Medicine and Dentistry, Moscow, Russia

⁶art photonics GmbH, Berlin, Germany

Correspondence

Ekaterina O. Bryanskaya, Research and Development Center of Biomedical Photonics, Orel State University, 95 Komsomolskaya st., Orel 302026, Russia.
Email: katrinbryanya@gmail.com

Funding information

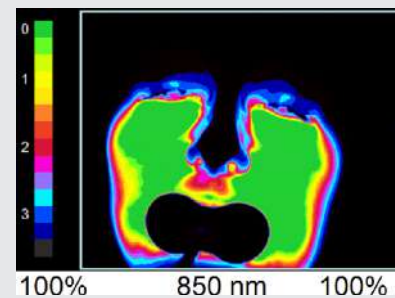
Foundation for Assistance to Small Innovative Enterprises in Science and Technology, Grant/Award Number: 353FC11ITC10-D5/80270; Russian Foundation for Basic Research, Grant/Award Number: 20-32-90147

Abstract

Maxillary sinus pathologies remain among the most common ENT diseases requiring timely diagnosis for successful treatment. Standard ENT inspection approaches indicate low sensitivity in detecting maxillary sinus pathologies. In this paper, we report on capabilities of digital diaphanoscopy combined with machine learning tools in the detection of such pathologies. We provide a comparative analysis of two machine learning approaches applied to digital diaphanoscopy data, namely, convolutional neural networks and linear discriminant analysis. The sensitivity and specificity values obtained for both employed approaches exceed the reported accuracy indicators for traditional screening diagnosis methods (such as nasal endoscopy or ultrasound), suggesting the prospects of their usage for screening maxillary sinuses alterations. The analysis of the obtained values showed that the linear discriminant analysis, being a simpler approach as compared to neural networks, allows one to detect the maxillary sinus pathologies with the sensitivity and specificity of 0.88 and 0.98, respectively.

KEYWORDS

convolutional neural networks, digital diaphanoscopy, linear discriminant analysis, maxillary sinuses, optical diagnostics



1 | INTRODUCTION

Nowadays, maxillary sinus diseases play an essential role in the socioeconomic situation in the world. The relevance of studying the problem of diagnosis of such diseases is due to a significant number of temporary and permanent disabilities [1]. There is an annual increase in

the incidence of respiratory organs in the world. Among patients hospitalized in ENT departments, the annual increase in patients with diseases of the nose and paranasal sinuses reaches more than 50%. Rhinological patients have become the main focus for ENT clinicians. Relapses in diseases after surgical treatment of sinusitis range from 20% to 60% [2, 3]. For example, in Russia, 10 million

people suffer from these diseases annually, 6.3 million people in Germany suffer from acute sinusitis and 2.6 million people from chronic sinusitis every year [4]. Sinusitis affects approximately 29 million adults in the United States annually [5]. Approximately 90% of patients with colds show a component of viral sinusitis [6]. Under the conditions of the COVID-19 pandemic, several studies were conducted, highlighting an increase in the development of diseases of the nasal mucosa, as well as of the paranasal sinuses caused by the disease [7].

Nasal endoscopy is an important technique for diagnosing sinusitis. However, this technique does not provide direct information on the condition of the maxillary sinuses (only indirect signs of sinusitis, such as hyperemia, swelling of the nasal mucosa on the affected side, narrowing of the lumen of the nasal passages) [8]. It is worth noting that the nasal endoscopy technique is characterized by painfulness for a patient and subjectivity of diagnosis. Ultrasound is an alternative diagnostic technique employed in ENT. The reports in the literature indicate that the diagnostic value of this technique in ENT applications is limited (low sensitivity and specificity), primarily due to low accuracy originating from the high occurrences of false-positive diagnoses [9]. The use of radiography and computed tomography (CT) in the nasolabial projection is limited due to radiation load on the patient [8].

Consequently, there is a need for a diagnostic method for fast differential diagnosis prospective for screening [10] that should not be as complex and expensive as radiography; computer or magnetic resonance imaging screening tools can serve to guide the decision-making process and the formulation of differential diagnoses, as well as to help identify early-stage disease processes for early identification and treatment [11].

Optical imaging techniques are a class of rapidly developing tools, among which digital diaphanoscopy is distinguished [12]. This technique is used in various fields of medicine [13], in particular, in ENT it is employed to detect pathological changes in the maxillary sinuses [14]. This technique is based on optical probing of the maxillary sinuses and the registration of diaphanograms. At the same time, there is no radiation load on the patient, on the contrary to CT use [15].

The method consists in probing the maxillary sinus with safe low-intensity radiation of the visible and near-infrared spectrum (650 and 850 nm). Normally, the maxillary sinus is a pneumatized cavity lined with a mucous membrane [16]. The probing radiation passing through the sinus is partially absorbed in the presence of pathological changes in the form of purulent contents, cystic fluid, tumor stretching, and so forth [8, 17, 18]. The presence of absorption is associated with high values of the

absorption coefficient of pathological areas at the probing wavelengths originated from high blood content or presence of absorbing exudates [19–21]. Subsequent registration of diaphanograms allows one to visualize the presence or absence of a pathological change [15].

Along with nasal endoscopy and ultrasound, diaphanoscopy is treated as a cost-effective diagnostic technique. The digital diaphanoscopy method provides an easy-to-use, convenient, and painless tool, allowing for direct interpretation of the diagnostic data. Digital diaphanoscopy can be used in telemedicine, as well as in population screening [10] to reveal a group of patients with pathologies among asymptomatic individuals.

Nowadays, conducted studies have shown the importance of not only quantifying the registered diaphanograms, but also developing a practical tool that allows real-time detection of maxillary sinus pathologies [14, 15]. Machine learning approaches have great potential in supporting this application. Quantitative parameters of the registered diaphanograms obtained earlier could be used as diagnostic criteria to build a classification model [22, 23], in particular utilizing linear discriminant analysis (LDA) [24]. In addition, the application of pattern recognition theory, namely convolutional neural networks (CNN), seems promising for the differentiation of the condition of the maxillary sinuses (presence or absence of pathology) due to the method's resistance to small shifts and rotations of objects in the input images possible during diagnostic procedure [25–27].

The purpose of this study is to consider the use of two classification methods, CNN and a classification model based on LDA, to detect maxillary sinus pathologies based on digital diaphanoscopy data.

2 | EXPERIMENTAL SYSTEM AND METHODOLOGY

Experimental studies were conducted in 49 conditionally healthy volunteers (13 male, 36 female, average age 20 ± 3 years old) and 42 patients of the Otorhinolaryngological Department of the clinical hospital with maxillary sinus diseases (20 male, 22 female, average age 49 ± 17 years old) using the previously developed digital diaphanoscopy device [14], with confirmation of the diagnosis for patients by reference methods (CT and/or MRI) [21]. The group of patients consisted of 12 patients with cystic fluid, 4 patients with mycetoma, 5 patients with polypus rhinosinusitis, 17 patients with chronic sinusitis, 1 patient with sinonasal papilloma, and 3 patients with curvature of the nasal septum.

The studies in patients were conducted on the basis of the ENT Department of the Clinical Center for

Maxillofacial, Reconstructive and Plastic Surgery of the University Clinic of the Yevdokimov A.I. Moscow State University of Medicine and Dentistry (Moscow, Russia). After receiving the description of the protocol, the volunteers signed an informed consent indicating their voluntary willingness to participate in the study. The study was approved by the Ethics Committee of the Orel State University (record of meeting No. 15 of February 21, 2019) and carried out in accordance with the 2013 Declaration of Helsinki by the World Medical Association.

During the study, the LED applicator of the diaphanoscopy device, operating at two probing wavelengths (650 and 850 nm), was placed into the patient's oral cavity. With the help of an LED applicator, the maxillary sinuses were probed and the subsequent registration of diaphanograms was carried out using a CMOS camera UI-3240CP-NIR-GL Rev.2 with a Pentax C1614-M (KP) lens (Pentax, Japan) located opposite the patient's face. A literary analysis of the spectral properties of maxillary sinuses and human head tissues in norm and pathology, as well as an analysis of previous studies on employment of the diaphanoscopy technique, showed that the use of 650 and 850 nm probing wavelengths is promising owing to relatively small absorption [14, 28, 29]. In addition, pathologies with an exudate component are better visualized at a wavelength of 850 nm, while for pathologies involving plethora a wavelength of 650 nm is preferable. In addition, a preliminary numerical simulation of the radiation propagation through the tissues of the maxillary sinus was carried out. The results obtained made it possible to justify the selected wavelengths as optimal for the study [30, 31]. Preliminary studies have shown that the recorded diaphanograms are strongly influenced by the value of the optical power of the LED applicator, which is due to the difference in the anatomical structure of the tissues of the maxillary sinuses in male and female (e.g., the thickness of the hypodermis, the size of the maxillary sinuses, etc.). In order to assess the influence of the optical power values, numerical simulation was carried out with the establishment of different values of the optical power for male and female. The choice of optical power values was carried out in accordance with the capabilities of the previously developed LED brightness controller of the digital diaphanoscope [32]. As a result, it was found that for female patients, the optimal optical power is 35/40 mW (650 nm) and 25/65 mW (850 nm), whereas for male patients, these values amount 55/60 mW (650 nm) and 80/85 mW (850 nm), respectively. The value of the camera exposure time was set to 40 ms. The LED applicator was disinfected before each study.

In the recorded diaphanograms of size of $N_x \times N_y$ ($N_x = 1280$, $N_y = 1024$), each point (pixel) corresponds to

the value of the light intensity that reached the camera detector after absorption and scattering in normal or/and pathological tissues of human head. Conclusion about the presence or absence of a pathological change was made based on spatial distribution of light detected by the camera, governed in particular by strong absorption at wavelengths of 650 and 850 nm in the maxillary sinus region with pathologies.

The specially designed software assists us in analyzing the obtained diaphanograms. It allows for control of the device operation (selection of a radiation source and a camera operation mode), recording diaphanograms, and their quantitative (visualization) and qualitative processing (pseudo-coloring). The pseudo-coloring consists in transforming of a diaphanogram $D(x,y)$ into a eight-bit image $I_{pc}(x,y)$ in accordance with formula:

$$I_{pc} = \frac{D(x,y) - \min_{x=1..N_x, y=1..N_y} D(x,y)}{\max_{x=1..N_x, y=1..N_y} D(x,y) - \min_{x=1..N_x, y=1..N_y} D(x,y)} \cdot 2^k, \quad (1)$$

where $k = 8$ is a bit characteristic of the image ($I_{pc}(x,y)$ is ranging from 0 to 255). Thus, depending on the degree of light absorption, pseudo-coloring makes it possible to better visualize the maxillary sinuses with the presence of a pathological change. For convenience, this image is presented in the percentage scale in accordance with formula:

$$\tilde{I}_{pc} = \frac{D(x,y) - \min_{x=1..N_x, y=1..N_y} D(x,y)}{\max_{x=1..N_x, y=1..N_y} D(x,y) - \min_{x=1..N_x, y=1..N_y} D(x,y)} \cdot 100\%. \quad (2)$$

3 | RESULTS AND DISCUSSION

3.1 | Clinical study

Figure 1 shows an example of a diaphanogram for a conditionally healthy volunteer. Figure 2 shows examples of study patients with chronic right-sided maxillary sinusitis (top) and with mycetoma of the right maxillary sinus (bottom), as well as the results of CT examination of the patients confirming the diagnosis.

The healthy sinus is airy due to absence of pathological change. Accordingly, the absorption of probing light in the right and left maxillary sinuses in norm is weak. This is confirmed by the results obtained for a conditionally healthy volunteer (Figure 1).

Patient with chronic right-sided maxillary sinusitis (Figure 2, top) complained of difficulty in nasal breathing, mainly on the right side, mucus draining into the

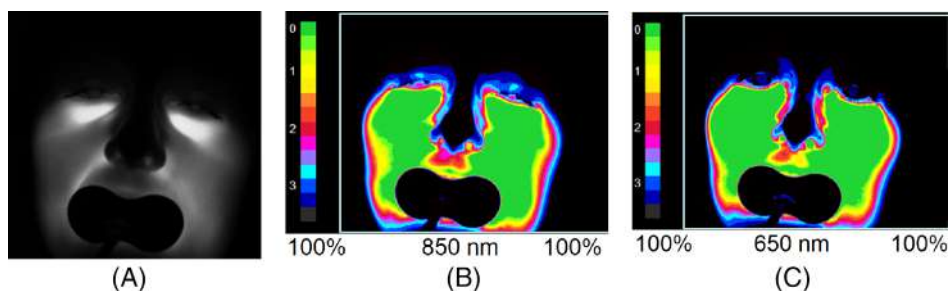


FIGURE 1 Typical diaphanoscopy examination results for a conditionally healthy volunteer: (A) registered diaphanogram, (B,C) results of pseudo-color image segmentation for probing radiation wavelengths of 850 and 650 nm, respectively.

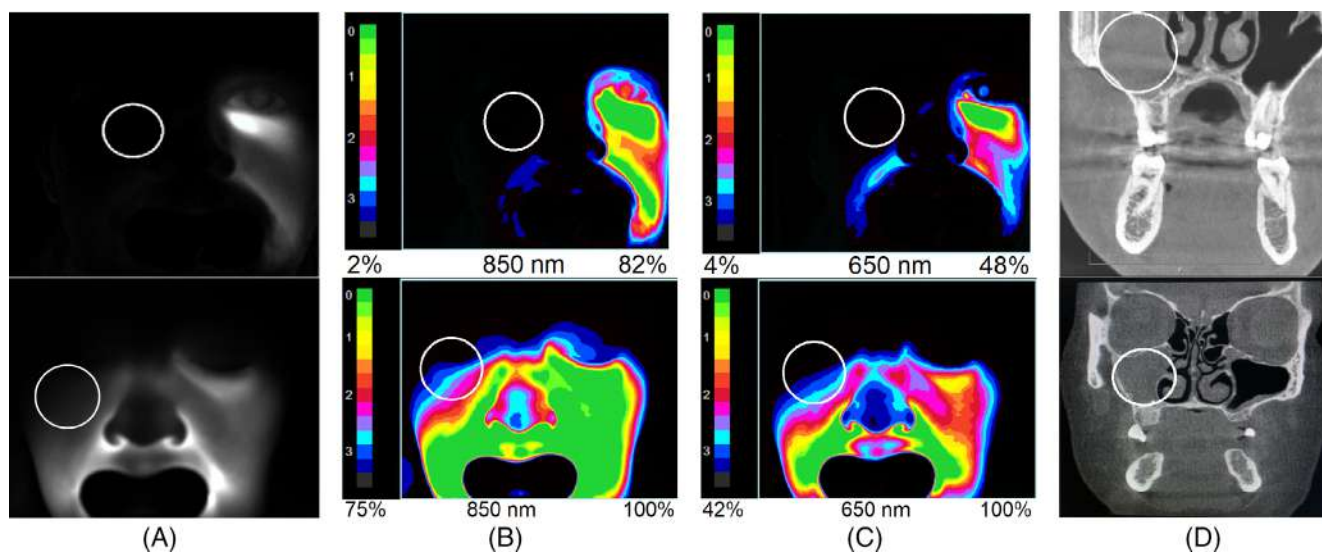


FIGURE 2 Typical diaphanoscopy examination results for patient with chronic right-sided maxillary sinusitis (top) and patient with mycetoma of the right maxillary sinus (bottom), where (A) registered diaphanograms, (B,C) results of pseudo-color image segmentation for probing radiation wavelengths of 850 and 650 nm, respectively, and (D) CT of the upper and lower jaws of the coronal plane. White circle indicates the area of pathology.

throat, symptoms are bothering for a long time, conservative treatment—without a pronounced positive effect. CT scan of the skull in the coronal projection shows a picture of chronic right-sided maxillary sinusitis, where the right maxillary sinus has total blackout, the remaining sinuses are airy.

Patient with mycetoma of the right maxillary sinus (Figure 2, bottom) complained of mucus flowing down the throat, discomfort in the right cheek area, symptoms have been bothering for a long time, conservative treatment was carried out without a pronounced positive effect. Examination by nasal endoscopy showed hyperemia of the nasal mucosa from the affected side, purulent discharge in the right middle nasal passage, and nasal breathing is difficult. CT scans of the upper and lower jaw in the coronal projection show that the right maxillary sinus has total blackout with inclusions of mycelium of the fungus, the remaining visible paranasal sinuses are airy.

In both examples for patients, the registered diaphanograms, as well as the results of pseudo-coloring, show a low-intensity region in the area of the right maxillary

sinuses, which indicates a decrease in its transparency and the presence of a pathological change. The left sinuses are normal for both patients. Consequently, the obtained CT results confirm the reliability and precision of digital diaphanoscopy as a screening technique, as well as the accuracy of the preliminary diagnosis.

3.2 | The application of convolutional neural networks

The automated classification system was developed on the basis of the CNN of the ResNet type [33] for solving the binary classification problem. The system was implemented in Python [34] using the FastAI framework [35] on the Google collaboration platform [36].

The ResNet34 network was used as a classification model. The input data was a set of RGB images with a resolution of 1280×1024 pixels, which at the stage of preparing the dataset were converted into images of 224×224 size. The total sample of the study consisted

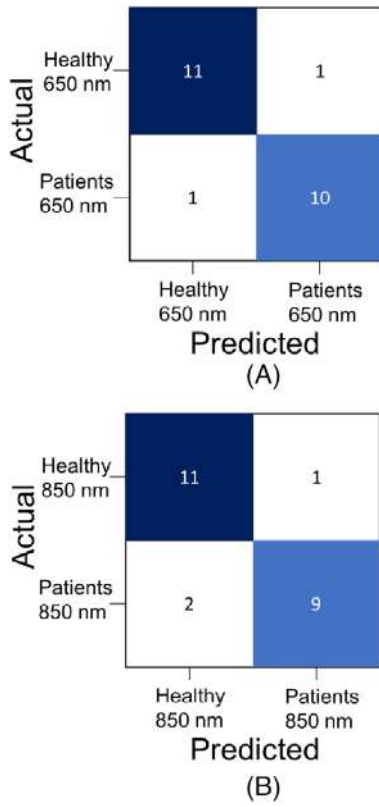


FIGURE 3 Confusion matrices for classification systems built using ResNet34 CNN for diaphanoscopy data obtained using a probing wavelength of (A) 650 nm and (B) 850 nm for the test sample.

of 91 persons (49 conditionally healthy volunteers and 42 patients), and the registration of diaphanograms was carried out for two probing wavelengths (650 nm and 850 nm). The division into test and training sets was carried out randomly, with proportion of 25%–75%. Cross-validation was not performed.

The framework [35] has a set of tools for image augmentation, including random crop with or without scaling (resizing), random rotation and flip, warping, random changing in brightness, contrast, and color representation, random erasing, and their combination [37]. The following values of augmentation tools parameters were used: minimum cropping scale (min_scale) of 0.6, maximum brightness change scale (max_lighting) of 0.4, and maximum deformation change value (max_warp) of 0.1. The classification model was built separately for the data obtained by probing the maxillary sinuses at a wavelength of 650 and 850 nm. The confusion matrices obtained for diaphanograms recorded at wavelengths of 650 and 850 nm for the test dataset are shown in Figure 3A,B, respectively.

In accordance with the presented confusion matrices, the accuracy parameters of the classification model were calculated.

The results obtained showed that the use of the 650 nm probing wavelength makes it possible to register diaphanograms with differentiation of the state of the sinuses into two classes (healthy and with pathological changes) with the following accuracy indicators: sensitivity of 0.91, and specificity of 0.92. For the case of maxillary sinuses probing with a wavelength of 850 nm, the sensitivity and specificity indicators were 0.82 and 0.92, respectively.

3.3 | The linear discriminant analysis application

In order to construct a classification model to divide the study objects into two classes (healthy and with inflammatory disease), the quantitative parameters of the registered diaphanograms, namely, asymmetry coefficient AC and intensity parameter I . To calculate I , the area of the maxillary sinus (ROI) is manually selected, in which the average value of the light intensity is calculated according to the formula:

$$I = \frac{\sum_{i=1..N} D_i}{N}, \quad (3)$$

where N is the number of pixels in the ROI.

The calculation of asymmetry coefficient AC consisted in determination of the face central line (symmetry axis), diaphanograms rotation to ensure vertical position of the central line, and calculating the asymmetry coefficient between the left and right parts of the face. The calculation was made according to formula:

$$AC = \frac{\sum_m \sum_n (A_{m,n} - \bar{A}) \cdot (B_{N_x/2-m,n} - \bar{B})}{\sqrt{\left(\sum_m \sum_n (A_{m,n} - \bar{A})^2\right) \cdot \left(\sum_m \sum_n (B_{m,n} - \bar{B})^2\right)}}, \quad (4)$$

where $A_{m,n} = D(x = 1..N_x/2, y = 1..N_y)$ and $B_{m,n} = D(x = N_x/2 + 1..N_x, y = 1..N_y)$ are pixel intensities in the left and right parts of the diaphanogram $D(x,y)$, respectively, \bar{A} and \bar{B} are the average intensities in the left and the right parts of the diaphanogram, respectively, m and n are indexes of columns and rows in diaphanogram parts $A_{m,n}$ and $B_{m,n}$.

Data analysis demonstrated a statistically significant difference between the calculated indicators for conditionally healthy volunteers and patients with pathological changes in the maxillary sinuses at $p < 0.05$ according to the Mann–Whitney criterion (Figure 4).

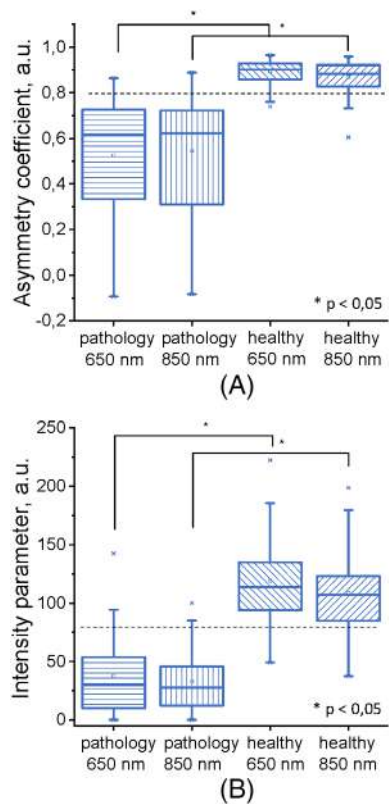


FIGURE 4 Intensity parameter (A) and asymmetry coefficient (B) for probing wavelengths of 650 and 850 nm calculated from diaphanoscopy data for healthy volunteers and patients with confirmed maxillary sinuses pathologies.

Based on the results obtained, the boundaries in the intensity parameter and asymmetry coefficient values for a healthy sinus and a sinus with pathology are clearly traced. LDA was chosen as an approach to construct the classification model [22]. The discriminant function can be represented in the following formula:

$$f(x) = k_1 \cdot I + k_2 \cdot AC + C, \quad (5)$$

where I and AC are the chosen diagnostic parameters for target groups, k_1 and k_2 are coefficients of the discriminant function, C is a free term (constant).

The first group is represented by conditionally healthy volunteers ($p_1 = 42$), the second group consists of patients with maxillary sinuses pathologies ($p_2 = 49$). Therefore, the initial sample was $m = p_1 + p_2 = 91$. To ensure the stability of the classifier and avoid over-fitting, leave-one-out cross-validation was used.

The LDA has shown that classification model providing the best values of sensitivity and specificity is described by the following canonical coefficients:

$$f(x) = (-0.07 \cdot I) + (-7.26 \cdot AC) + 9.85. \quad (6)$$

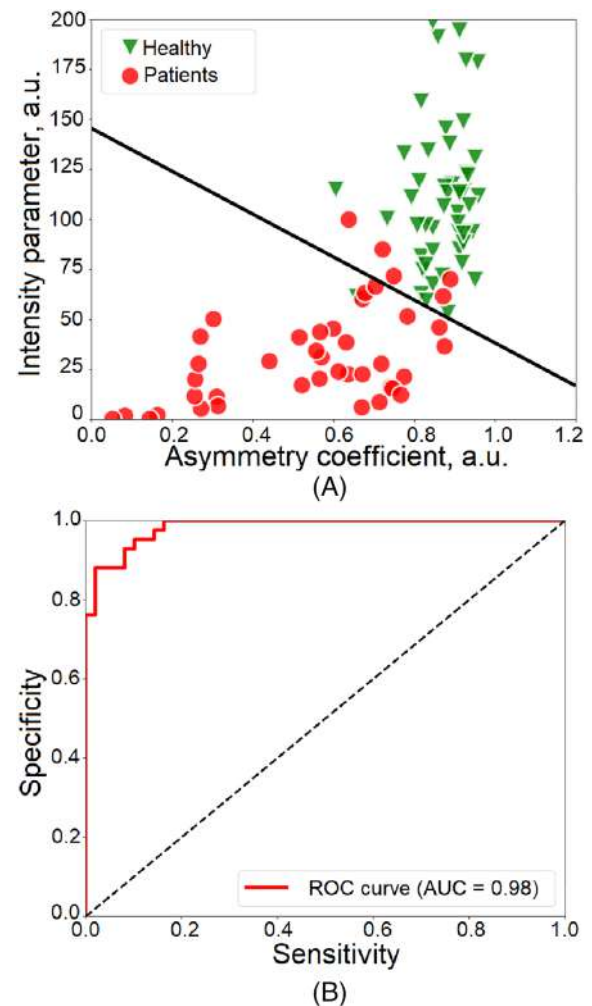


FIGURE 5 The scatter plot with applied discriminant line obtained by linear discriminant analysis method (A) and ROC curve (B).

where I and AC are the values of the intensity parameter and the asymmetry coefficient, respectively.

Visual representation of this model performance is shown in Figure 4 for probing wavelength of 850 nm with applied discriminant line that divides the experimental points into two groups (healthy volunteers and patients).

The obtained results showed that the sensitivity and specificity values for the probing wavelength of 850 nm are 0.88 and 0.98, respectively. For the case of probing the maxillary sinuses with a wavelength of 650 nm, the sensitivity and specificity are 0.81 and 0.98, respectively. The obtained values indicate a high level of efficiency of the synthesized classification model (Figure 5). At the same time, a high specificity rate is characteristic of screening methods [10].

The digital diaphanoscopy also has high potential in quantitative evaluation of maxillary sinuses pathologies.

TABLE 1 Comparison of cost-effective approaches to the diagnosis of diseases of the maxillary sinuses.

Diagnostic method	Nasal endoscopy [38–41]	Ultrasound [9, 42–44]	Diaphanoscopy and CNN		Diaphanoscopy and LDA	
			650	850	650	850
Probing wavelength, nm	–	–	650	850	650	850
Sensitivity	0.21–0.69	0.32–0.64	0.91	0.82	0.81	0.88
Specificity	0.66–0.80	0.53–0.95	0.92	0.92	0.98	0.98
Accuracy	0.61–0.80	0.32–0.56	0.92	0.84	0.90	0.91

Abbreviations: CNN, convolutional neural networks; LDA, linear discriminant analysis.

In this study, the calculation of quantitative parameters, such as the asymmetry coefficient and the intensity parameter, allows to produce a binary classification of the maxillary sinuses conditions based on machine learning methods. However, quantitative assessment has prospects in the pathology's differential diagnosis, for example, further machine learning approaches could help in characterizing of severity of the maxillary sinuses pathology given larger training set of diaphanoscopy data with a predefined severity evaluations made by ENT specialists. The development of a decision-making support system for diaphanoscopy seems promising to perform rapid diagnosis of maxillary sinuses diseases, for population screening, as well as for telemedicine.

At the same time, reasonable diagnostic criteria should be included in classification model. This model should form the basis of the software and feature a high level of accuracy of diagnosis, namely, the accuracy indicators should exceed those of the currently employed cost effective diagnostic techniques, such as nasal endoscopy, or ultrasound.

According to the literature data, the nasal endoscopy method, which is also a cost-effective diagnostic method, allows diagnosing diseases with sensitivity of 0.21–0.69 and specificity of 0.66–0.80. The ultrasound method has sensitivity of 0.32–0.64 and specificity of 0.53–0.95. At the same time, the results obtained showed prospects of application of a diagnostic system based on CNN and a classification model based on LDA for the screening of the population, dividing the group of asymptomatic individuals into two classes depending on the absence and presence of maxillary sinus inflammatory disease. However, the use of the second approach is simpler, and thus it can be chosen as an approach to assist in the digital diaphanoscopy technology. When using this approach, it is possible to obtain sensitivity value of 0.88 and specificity value of 0.98.

Table 1 summarizes the diagnostic accuracy parameters for nasal endoscopy, ultrasound, and digital diaphanoscopy in particular based on data reported in [9, 38–44]. A significant exceed of the values for diaphanoscopy over those for nasal endoscopy and ultrasound indicates

high potential of diaphanoscopy in both fast diagnostics of maxillary sinuses and screening performance.

4 | CONCLUSION

By comparison of two machine learning approaches to build classification models for determination maxillary sinuses pathologies in digital diaphanoscopy, we have developed a new practical tool for diagnosing and screening this type of alterations.

The article considers the application of two different classification methods: CNN and LDA. The obtained results showed that the use of CNN makes it possible to accurately enough detect the presence of pathological changes. However, in this case, only registered diaphanograms were considered to calculate the diagnostic accuracy characteristics, and the values obtained depend on the specified parameters of the CNN. The use of LDA allows one to simplify the problem, since in this case, the analysis of secondary features is performed (quantitative parameters calculated from the obtained diaphanograms) and the dimensionality of the problem is significantly decreased. Therefore, the classification model based on a LDA allows for high-accuracy detection of pathology presence with the sensitivity and specificity indicators being 0.88 and 0.98, respectively. This analysis allows one to significantly reduce the probability of a false-negative result in comparison to traditional approaches.

In the future, this model will be actualized by dataset increase. So, the model can be used to improve the software of the digital diaphanoscope, and to develop a system to support medical decision-making.

ACKNOWLEDGMENTS

This study was funded by RFBR according to the research project No. 20-32-90147 and by FASIE according to the project No. 353FC1IITC10-D5/80270. Thanks to the volunteers and patients of the University Clinic of the Yevdokimov A.I. Moscow State University of Medicine and Dentistry (Moscow, Russia).

CONFLICT OF INTEREST STATEMENT

The authors declare no conflicts of interest.

DATA AVAILABILITY STATEMENT

Data will be made available on request.

ORCID

Ekaterina O. Bryanskaya  <https://orcid.org/0000-0002-2950-4443>

Viktor V. Dremine  <https://orcid.org/0000-0001-6974-3505>

Valery V. Shupletsov  <https://orcid.org/0009-0006-0024-8518>

Alexey V. Kornaeve  <https://orcid.org/0000-0001-5121-6045>

Mikhail Yu. Kirillin  <https://orcid.org/0000-0002-6804-6369>

Anna V. Bakotina  <https://orcid.org/0000-0003-2750-6899>

Dmitry N. Panchenkov  <https://orcid.org/0000-0001-8539-4392>

Konstantin V. Podmasteryev  <https://orcid.org/0000-0002-1626-994X>

Viacheslav G. Artyushenko  <https://orcid.org/0000-0003-4592-3936>

Andrey V. Dunaev  <https://orcid.org/0000-0003-4431-6288>

REFERENCES

- [1] S. A. Fong, A. Drilling, S. Morales, M. E. Cornet, B. A. Woodworth, W. J. Fokkens, A. J. Psaltis, S. Vreugde, P.-J. Wormald, *Front Cell Infect Microbiol* **2017**, *7*, 1.
- [2] S. E. Smith, R. J. Schlosser, J. R. Yawn, J. L. Mattos, Z. M. Soler, J. K. Mulligan, *Am. J. Rhinol. Allergy* **2017**, *31*, 352.
- [3] B. R. Haxel, P. Boessert, V. Weyer-Elberich, K. Fruth, *Laryngo-scope Investig. Otolaryngol.* **2017**, *2*, 269.
- [4] Gesundheitsberichterstattung des bundes. gemeinsam getragen von rki und destatis. https://www.gbe-bund.de/gbe/pkg_isgbe5.prc_isgbe **2022**.
- [5] M. Villarroel, D. Blackwell, A. Jen, Tables of Summary Health Statistics for U.S. Adults: 2018 National Health Interview Survey, National Center for Health Statistics, 1–9 (2019).
- [6] A. S. Battisti, P. Modi, J. Pangia, *Sinusitis. StatPearls—NCBI Bookshelf*, StatPearls, Treasure Island, FL **2022**.
- [7] Y. Yamazaki, Kosaka M, Maruno T, Shimizu S, Sakaguchi K., *Kansenshogaku zasshi. The Journal of the Japanese Association for Infectious Diseases* **2020**, *94*(4), 583–586.
- [8] A. Al-Qahtani, H. Haidar, A. Larem, *Textbook of Clinical Otolaryngology*, Springer Nature, New York City **2021**.
- [9] C. C. Hsu, C. Sheng, C. Y. Ho, *J. Chinese Med. Assoc.* **2018**, *81*, 898.
- [10] A. Sagan, D. McDaid, S. Rajan, J. Farrington, M. McKee, *Screening. When is it appropriate and how can we get it right*, Health Systems and Policy Analysis, World Health Organization, Denmark **2020**.
- [11] J. Conigliaro, S. Kapoor, *Handbook of Outpatient Medicine*, Springer, Cham **2023**, p. 3.
- [12] A. V. Dunaev. *Proc. SPIE* **2022**, *12192*, 121920T.
- [13] F. H. J. Koch, S. Deuchler, M. Hessling, P. Singh, *Der Ophthalmol.* **2017**, *11*, 331.
- [14] U. J. Zabarylo. Methodische Untersuchungen zur Bildbearbeitung von diaphanoskopischen Streulichtbildern und deren Fusion mit anderen Modalitäten der Bildgebung. Doctoral Dissertation **2021**.
- [15] E. O. Bryanskaya, I. N. Novikova, V. V. Dremine, R. Y. Gneushev, O. A. Bibikova, A. V. Dunaev, V. G. Artyushenko, *Diagnostics* **2021**, *11*, 1.
- [16] P. S. Batista, A. F. Do Rosário Junior, C. Wichneski, *A contribution to the maxillary sinus study*, Vol. 52, Revista Portuguesa de Estomatologia, Medicina Dentaria e Cirurgia Maxilofacial, Lisboa **2011**, p. 235.
- [17] J. Kastner, J. Lisy, M. Taudy, P. Grabec, J. Betka, *Rhinology* **2010**, *48*, 457.
- [18] K. Sato, S. I. Chitose, K. Sato, F. Sato, T. Ono, H. Umeno, *Laryngoscope Investig. Otolaryngol.* **2020**, *5*, 205.
- [19] V. G. Peters, D. R. Wymant, M. S. Patterson, G. L. Frank, *Phys. Med. Biol. Relat. Content* **1990**, *35*, 1317.
- [20] R. L. P. Van Veen, H. J. C. M. Sterenborg, A. W. K. S. Marinelli, M. Menke-Pluymers, *J. Biomed. Opt.* **2004**, *9*, 1129.
- [21] S. L. Jacques, *Phys. Med. Biol.* **2013**, *58*, 37.
- [22] E. O. Bryanskaya, I. N. Novikova, V. V. Dremine, Y. O. Nikolaeva, V. G. Pil'nikov, A. V. Bakotina, A. Y. Ovchinnikov, D. N. Panchenkov, A. V. Baranov, V. G. Artyushenko, A. V. Dunaev. *Proc. SPIE* **2022**, *12192*, 121920A.
- [23] E. O. Bryanskaya, V. V. Dremine, I. N. Novikova, Y. O. Nikolaeva, V. G. Pil'nikov, A. V. Bakotina, A. Y. Ovchinnikov, D. N. Panchenkov, A. V. Baranov, V. G. Artyushenko, A. V. Dunaev, *2022 Int. Conf. Laser Opt. ICLO 2022—Proceedings, IEEE*, **2022**, 1–1.
- [24] A. V. Dunaev. Multiparameter optical methods and instruments for the diagnostics of human body microcirculatory-tissue systems," Proceedings of SPIE (11845), 1184505. **2021**.
- [25] I. N. Stebakov, E. P. Kornaeve, E. V. Potapova, V. V. Dremine. Application of shallow and deep convolutional neural networks to recognize the average flow rate of physiological fluids in a capillary," *Proc. SPIE* (121940), 121940D. **2022**.
- [26] E. P. Kornaeve, I. N. Stebakov, A. V. Kornaeve, V. V. Dremine, S. G. Popov, A. Y. Vinokurov, *Int J Mech Sci* **2023**, *242*, 107967.
- [27] K. He, X. Zhang, S. Ren, J. Sun, *Proc IEEE Comput Soc Conf Comput Vis Pattern Recognit*, IEEE Computer Society, 1–12 (2015).
- [28] M. Hopf, J. U. G. Hopf, *Med. Laser Appl.* **2003**, *18*, 217.
- [29] M. F. Mafee, N. Farid, W. Y. Lim, *Diseases of the Sinuses* (Eds: C. C. Chang, G. A. Incaudo, M. Eric Gershwin), Springer, New York, NY (2014).
- [30] E. O. Bryanskaya, G. R. Yu, I. N. Makovik, V. V. Dremine, A. G. Bukin, O. A. Bibikova, B. M. Shuraev, O. Minet, U. Zabarylo, A. V. Dunaev, V. G. Artyushenko. *Proc. SPIE Proc SPIE* **2020**, *11457*, 114571K.
- [31] E. O. Bryanskaya, G. R. Yu, I. Novikova, V. Dremine, A. Dunaev, *Proc. SPIE* **2021**, *11845*, 118450U.
- [32] E. O. Bryanskaya, R. Y. Gneushev, I. N. Novikova, V. V. Dremine, A. V. Dunaev. "Brightness controller optimization for

- the digital diaphanoscopy system,” European Conferences on Biomedical Optics 2021 (ECBO), ETu2A.3. **2021**.
- [33] Python.org, <https://www.python.org/> (2001–2022).
- [34] Fast.ai. Making neural nets uncool again. <https://www.fast.ai/> **2016–2022**.
- [35] Colaboratory, <https://colab.research.google.com/notebooks/intro.ipynb> **2022**.
- [36] ImageNet, <https://www.image-net.org/> **2020–2022**.
- [37] fast.ai. Vision augmentation. <https://docs.fast.ai/vision.augment.html> **2016–2022**.
- [38] A. Aysel, A. M. Koç, M. E. Zorlu, O. Yıldırım, T. Muderris, *Eur. J. Rhinol. Allergy* **2021**, 4, 77.
- [39] K. Nathan, S. K. Majhi, R. Bhardwaj, A. Gupta, S. Ponnusamy, C. Basu, A. Kaushal, *Sinusitis* **2021**, 5, 59.
- [40] S. Chainansamit, C. Chit-uea-ophat, W. Reechaipichitkul, P. Piromchai, *Ear, Nose Throat J.* **2021**, 100, 167.
- [41] E. Günbey, H. P. Günbey, S. Uygun, H. Karabulut, C. Cingi, *Int. Forum Allergy Rhinol.* **2015**, 5, 839.
- [42] K. Laine, T. Määttä, H. Varonen, M. Mäkelä, *Rhinology* **1998**, 36, 2.
- [43] T. Puhakka, T. Heikkinen, M. J. Mäkelä, A. Alanen, T. Kallio, L. Korsoff, J. Suonpää, O. Ruuskanen, *Arch. Otolaryngol. Neck Surg.* **2000**, 126, 1482.
- [44] A. Valkov, G. Nikolov, B. Duhlenki, T. Stoyanov, T. Mladenov, M. Yildiz, K. Atanasova, S. Mirchev, K. Valcheva, *Int. Bull. Otorhinolaryngol.* **2021**, 17, 40.

How to cite this article: E. O. Bryanskaya, V. V. Dremin, V. V. Shupletsov, A. V. Kornaev, M. Y. Kirillin, A. V. Bakotina, D. N. Panchenkov, K. V. Podmasteryev, V. G. Artyushenko, A. V. Dunaev, *J. Biophotonics* **2023**, e202300138. <https://doi.org/10.1002/jbio.202300138>